



HAL
open science

The TBP associated factor "yTaf II 19p" functionally interacts with components of the global transcriptional regulator "the Ccr4-Not complex" and physically interacts with the Not5 subunit

Marc Lemaire, Martine A Collart

► **To cite this version:**

Marc Lemaire, Martine A Collart. The TBP associated factor "yTaf II 19p" functionally interacts with components of the global transcriptional regulator "the Ccr4-Not complex" and physically interacts with the Not5 subunit. *Journal of Biological Chemistry*, 2000, 275 (35), pp.26925-26934. 10.1074/jbc.M002701200 . hal-01632826

HAL Id: hal-01632826

<https://hal.science/hal-01632826>

Submitted on 10 Nov 2017

HAL is a multi-disciplinary open access archive for the deposit and dissemination of scientific research documents, whether they are published or not. The documents may come from teaching and research institutions in France or abroad, or from public or private research centers.

L'archive ouverte pluridisciplinaire **HAL**, est destinée au dépôt et à la diffusion de documents scientifiques de niveau recherche, publiés ou non, émanant des établissements d'enseignement et de recherche français ou étrangers, des laboratoires publics ou privés.

The TATA-binding Protein-associated Factor γ Taf_{II}19p Functionally Interacts with Components of the Global Transcriptional Regulator Ccr4-Not Complex and Physically Interacts with the Not5 Subunit*

Received for publication, March 28, 2000, and in revised form, May 31, 2000
Published, JBC Papers in Press, June 22, 2000, DOI 10.1074/jbc.M002701200

Marc Lemaire[‡] and Martine A. Collart[§]

From the Département de Biochimie Médicale, Centre Médical Universitaire, 1 rue Michel Servet, 1211 Geneva 4, Switzerland

The *Saccharomyces cerevisiae* *HIS3* gene is a model system to characterize transcription initiation from different types of core promoters. The *NOT* genes were identified by mutations that preferentially increased transcription of the *HIS3* promoter lacking a canonical TATA sequence. They encode proteins associated in a complex that also contains the Caf1 and Ccr4 proteins. It has been suggested that the Ccr4-Not complex represses transcription by inhibiting factors more specifically required for promoters lacking a TATA sequence. A potential target is the γ Taf_{II}19 subunit of TFIID, which, when depleted, leads to a preferential decrease of *HIS3* TATA-less transcription. We isolated conditional *taf19* alleles that display synthetic growth phenotypes when combined with *not4* or specific *not5* alleles. Inactivation of γ Taf_{II}19p by shifting these mutants to the restrictive temperature led to a more rapid and striking decrease in transcription from promoters that do not contain a canonical TATA sequence. We demonstrated by the two-hybrid assay and directly *in vitro* that γ Taf_{II}19p and Not5p could interact. Finally, we found by the two-hybrid assay that γ Taf_{II}19p also interacted with many components of the Ccr4-Not complex. Taken together, our results provide evidence that interactions between Not5p and γ Taf_{II}19p may be involved in transcriptional regulation by the Ccr4-Not complex.

Transcription initiation by RNA polymerase II involves the assembly of a functional preinitiation complex on the core promoter (1). An essential step in this assembly is the recognition of the core promoter by general transcription factors. The TBP¹ subunit of TFIID plays a crucial role in this recognition event for TATA-containing promoters (2). For promoters that do not contain canonical TATA sequences (referred as TATA-less), other factors probably contribute to the correct positioning of the polymerase. Biochemical analyses indicate that the Taf_{II} subunits of TFIID make extensive contacts to the core

promoter independently of the TATA element (3). This has implicated Taf_{II}s themselves in participating in the core promoter recognition event and has suggested that Taf_{II}s might be particularly important for recognition of TATA-less core promoters. In any event, this would define the general transcription factor TFIID as being the key player in core promoter recognition.

However, the role and mechanisms of action of the Taf_{II}s still remain unclear. Recently Taf_{II}-containing complexes distinct from TFIID have been described in mammalian cells and in yeast (4–7). These complexes share some but not all TFIID Taf_{II} subunits. One example is the yeast SAGA histone acetyltransferase complex. These findings might call into question the presence of TFIID at all promoters. It could be that other Taf_{II}-containing complexes function at some promoters. Such a possibility has been further supported by studies of the *in vivo* role of many Taf_{II}s in yeast (for reviews, see Refs. 8 and 9). Indeed, it appears that some Taf_{II}s may be generally required for transcription (such as γ Taf_{II}17_{HP}), whereas others function only at some core promoters (such as γ Taf_{II}145_{HP}).

To understand in detail the mechanism of transcription initiation at TATA-less promoters, *in vitro* studies have not been very useful, because transcription initiation from promoters that lack both a TATA box and an initiator sequence is usually inefficient. In yeast, the *HIS3* gene has been used as a model to investigate the differences between TATA-containing and TATA-less core promoter transcription initiation. Indeed, the *HIS3* promoter contains both types of core promoters, which are functionally distinguishable (10, 11), because activation by upstream bound activators only functions through the TATA promoter. In Taf_{II} depletion assays, transcription from the *HIS3* TATA-less promoter has been shown to decrease preferentially in some cases. This has led to the suggestion that γ Taf_{II}19p, γ Taf_{II}145p, γ Taf_{II}40p, and γ Taf_{II}67p are more specifically required for TATA-less transcription (12, 13). In contrast, recent work has suggested that in fact γ Taf_{II}40p is generally required for transcription by RNA polymerase II (14). γ Taf_{II}40p and γ Taf_{II}19p are the yeast homologues of huTaf_{II}28p and huTaf_{II}18p, two subunits of the human TFIID complex interacting via histone-fold dimerization domains (15). γ Taf_{II}145p is the yeast homologue of huTaf_{II}250 and was presumed to be the TFIID scaffold, although this belief has been challenged by recent work (discussed in Ref. 9). Not much has been described about γ Taf_{II}67p.

In other studies, the five *NOT* genes have been identified by mutations that increase *HIS3* transcription. The Not proteins preferentially repress transcription from the *HIS3* TATA-less promoter and have been described as global regulators of transcription, as they also affect the transcription of many unrelated genes (16–18). The Not proteins are associated in one or

* This work was supported by Swiss National Science Foundation Grants 31-39690.93 and 31-49808.96 (to M. A. C.) and by Grant OFES96.0072 TMR (to M. A. C.). The costs of publication of this article were defrayed in part by the payment of page charges. This article must therefore be hereby marked "advertisement" in accordance with 18 U.S.C. Section 1734 solely to indicate this fact.

[‡] Present address: Université Claude Bernard, Unité de Microbiologie et Génétique, Génétique des Levures, Bt 405 R2, 43 Boulevard du 11 Novembre 1918, 69622 Villeurbanne Cedex, France.

[§] To whom correspondence should be addressed. Tel.: 41-22-702-55-16; Fax: 41-22-702-55-02; E-mail: martine.collart@medecine.unige.ch.

¹ The abbreviations used are: TBP, TATA-binding protein; PCR, polymerase chain reaction; ORF, open reading frame; GST, glutathione S-transferase; PAGE, polyacrylamide gel electrophoresis; TFIID, transcription factor IID.

TABLE I
Yeast strains

Strains	Genotype	Source
MY1	<i>Mata ura3-52 trp1-1 leu2::PET56 gal2 gcn4-Δ1</i>	Ref. 35
MY2	Isogenic to MY1 except <i>MATα</i>	Ref. 18
MY4	Isogenic to MY2 except <i>his3::TRP1</i>	This work
MY542	Diploid MY1 × MY4	This work
MLY192	Isogenic to MY1 except <i>not4-1 taf19::KanMX4</i> + pMAC195	This work
MLY242	Isogenic to MY1 except <i>not4-1 taf19::KanMX4</i> + pML25	This work
MLY243	Isogenic to MY1 except <i>not4-1 taf19::KanMX4</i> + pML64	This work
MLY244	Isogenic to MY1 except <i>not4-1 taf19::KanMX4</i> + pML65	This work
MLY245	Isogenic to MY1 except <i>not4-1 taf19::KanMX4</i> + pML66	This work
MLY175	Isogenic to MY542 except <i>TAF19/taf19::KanMX4</i>	This work
MLY184	Isogenic to MLY175 but carrying pMAC195	This work
MLY187	Isogenic to MY1 except <i>taf19::KanMX4</i> + pMAC195	This work
MLY204	Isogenic to MY2 except <i>taf19::KanMX4</i> + pMAC195	This work
MLY268	Isogenic to MY1 except <i>taf19::KanMX4</i> + pML25	This work
MLY270	Isogenic to MY1 except <i>taf19::KanMX4</i> + pML64	This work
MLY272	Isogenic to MY1 except <i>taf19::KanMX4</i> + pML65	This work
MLY274	Isogenic to MY1 except <i>taf19::KanMX4</i> + pML66	This work
YOU584	Isogenic to MY2 except <i>not4::LEU2</i>	Ref. 16
MLY297	Isogenic to MY2 except <i>not4::LEU2 taf19::KanMX4</i> + pMAC195	This work
MLY365	Isogenic to MY2 except <i>not4::LEU2 taf19::KanMX4</i> + pML25	This work
MLY367	Isogenic to MY2 except <i>not4::LEU2 taf19::KanMX4</i> + pML64	This work
MLY369	Isogenic to MY2 except <i>not4::LEU2 taf19::KanMX4</i> + pML26	This work
MY1719	Isogenic to MY2 except <i>not5::LEU2</i>	Ref. 16
MLY309	Isogenic to MY2 except <i>not5::LEU2 taf19::KanMX4</i> + pMAC195	This work
MLY329	Isogenic to MY2 except <i>not5::LEU2 taf19::KanMX4</i> + pML25	This work
MLY331	Isogenic to MY2 except <i>not5::LEU2 taf19::KanMX4</i> + pML64	This work
MLY333	Isogenic to MY2 except <i>not5::LEU2 taf19::KanMX4</i> + pML66	This work
YOU123	Isogenic to MY1 except <i>not5-1</i>	Ref. 16
MLY321	Isogenic to MY2 except <i>not5-1 taf19::KanMX4</i> + pMAC195	This work
MLY347	Isogenic to MY2 except <i>not5-1 taf19::KanMX4</i> + pML25	This work
MLY349	Isogenic to MY2 except <i>not5-1 taf19::KanMX4</i> + pML64	This work
MLY351	Isogenic to MY2 except <i>not5-1 taf19::KanMX4</i> + pML66	This work
YOU142	Isogenic to MY2 except <i>not5-2</i>	Ref. 16
MLY323	Isogenic to MY1 except <i>not5-2 taf19::KanMX4</i> + pMAC195	This work
MLY353	Isogenic to MY1 except <i>not5-2 taf19::KanMX4</i> + pML25	This work
MLY355	Isogenic to MY1 except <i>not5-2 taf19::KanMX4</i> + pML64	This work
MLY357	Isogenic to MY1 except <i>not5-2 taf19::KanMX4</i> + pML66	This work
MY2268	Isogenic to MY2 except <i>taf19::KanMX4</i> + pML70	This work
MY2269	Isogenic to MY2 except <i>taf19::KanMX4</i> + pML71	This work
MY2270	Isogenic to MY2 except <i>taf19::KanMX4</i> + pML70 + pML136	This work
MY2271	Isogenic to MY2 except <i>taf19::KanMX4</i> + pML71 + pML136	This work
EGY48	<i>MATα trp1 ura3 his3 LEU2::pLEXAop6-LEU2</i>	Ref. 25

multiple large complexes (16) that also contain the Ccr4 and Caf1 proteins, known to be required for nonfermentative gene expression (19). It has been suggested that the Ccr4-Not complex might function to repress transcription of TATA-less promoters by sequestering or inhibiting factors more specifically required for TATA-less transcription (18). A putative target of the Ccr4-Not complex is TFIID (or some of its subunits) because of its probable implication in core promoter recognition. At the present time, there is no experimental evidence to support this model. Not1p has been reported to co-immunoprecipitate with TBP (20), but other experiments have shown that transcriptional activity resulting from a functional Spt3p-TBP interaction is a target for repression by the Not1p (21). Furthermore, interactions between Not2p and the Ada proteins have also been reported (22). Taken together, these results might point to the SAGA complex rather than TFIID.

To further understand the mechanisms involved in transcription regulation by the Ccr4-Not complex, we sought to investigate whether yTaf_{II}19p, a TFIID subunit apparently preferentially required for transcription of the *HIS3* TATA-less promoter, interacted in any way with the Ccr4-Not complex. Our interest in yTaf_{II}19p in particular was raised partly from the observations that (i) Spt3p and yTaf_{II}19p carry homologous sequences (15) and are thought to play similar roles in the SAGA and TFIID complexes, respectively (discussed in Ref. 9), and (ii) Spt3p appears to be a target for transcriptional regulation by the Ccr4-Not complex (21). We isolated temperature-sensitive *taf19* alleles and found that they displayed, at

permissive temperature, striking synthetic slow growth phenotypes with *not4* and *not5* mutants on minimal medium. In particular, two *not5* alleles encoding truncated proteins of different lengths behaved differently when combined with mutant *taf19* alleles but not with wild type *TAF19*. This suggested that yTaf_{II}19p and Not5p might interact, a hypothesis that could be confirmed both by two-hybrid experiments and by a direct interaction between Not5p and yTaf_{II}19p *in vitro*. Our results provide the first evidence that adequate transcription regulation by the Ccr4-Not complex may involve interactions with TFIID Taf_{II}s.

EXPERIMENTAL PROCEDURES

Strains and Media—All strains are described in Table I and were generated by classical genetic techniques. Media were standard. Strains carrying the kanMX4 module were selected for on YPD plates supplemented with G418 (200 mg/l, Life Technologies). *Escherichia coli* DH5α and BL21 (DE3) were used as cloning host and for recombinant protein expression, respectively.

TAF19 Gene Disruption—*TAF19* complete disruption was obtained through homologous recombination by transformation of PCR¹-synthesized marker cassettes with long flanking homology regions into MY542 (23). Briefly, by using two consecutive PCRs, upstream and downstream regions of *TAF19* (containing start and stop codons, respectively) were placed at each end of the selectable kanMX4 cassette from pFA6a-kanMX4. The primers used for the *TAF19* long flanking homology-PCR synthesis were as follows: P5', 5'-AAA AGT CGA CTC CTC TGC ACG TCC AAC ACC C-3' (the *HincII* site is underlined; the region starting 304 base pair upstream of the *TAF19* start codon is in boldface); P5'L, 5'-GGG GAT CCG TCG ACC TGC AGC GTA CGC ATA TCT TAT CCA GCT CAC CC-3' (the reverse complement of the

TABLE II
Plasmids

Plasmids	Description	Source
pMAC186	pUCBM21 derivative carrying the <i>TAF19</i> ORF	This work
pML49	<i>TRP1</i> centromeric plasmid carrying <i>TAF19</i>	This work
pMAC197	pET15b derivative carrying <i>TAF19</i>	This work
pMAC253	pET15b derivative carrying <i>CCR4</i>	This work
pMAC195	<i>URA3</i> centromeric plasmid carrying <i>TAF19</i> under the <i>DED1</i> promoter control	This work
pML25	pPC86 derivative carrying <i>TAF19</i> under the <i>ADC1</i> promoter control	This work
pML64	pPC86 derivative carrying <i>taf19-1</i> under the <i>ADC1</i> promoter control	This work
pML65	pPC86 derivative carrying <i>taf19-7</i> under the <i>ADC1</i> promoter control	This work
pML66	pPC86 derivative carrying <i>taf19-9</i> under the <i>ADC1</i> promoter control	This work
pML69	pPC62 derivative carrying <i>TAF19</i> under the <i>ADC1</i> promoter control	This work
pML70	pPC62 derivative carrying <i>taf19-1</i> under the <i>ADC1</i> promoter control	This work
pML71	pPC62 derivative carrying <i>taf19-9</i> under the <i>ADC1</i> promoter control	This work
pML98	pLEX202 derivative carrying <i>LexA-TAF19</i> fusion	This work
pML132	pLEX202 derivative carrying <i>LexA-taf19-7</i> fusion	This work
pML133	pLEX202 derivative carrying <i>LexA-taf19-9</i> fusion	This work
pML135	pLEX202 derivative carrying <i>LexA-taf19-1</i> fusion	This work
pMPM272	pMPM-A4 derivative expressing GST under the control of the <i>AraC</i> promoter	This work
pML136	<i>TRP1</i> multicopy plasmid carrying <i>TAF40</i>	This work
pML63	pMPM272 derivative expressing GST-yTaf _{II} 19p	This work
pU61	pET15b/22b derivative expressing His ₆ Not5p	This work

TAF19 start codon is in boldface and underlined; the *TAF19* 5' upstream region is in boldface; and the kanMX4 region is in plain text); P3'L, 5'-AAA CGA GCT CGA ATT CAT CGA TGA TAT GAT ATA GCT ACT TGG CAG GC-3' (the *TAF19* stop codon is in boldface and underlined; the *TAF19* 3' downstream region is in boldface; and the kanMX4 region is in plain text); and P3', AAA ACT GCA GTA GGA GGC GCA CGT ACC TTC C (the *PstI* site is underlined; the region starting 398 base pair downstream of the *TAF19* stop codon is in boldface). Correct integrations were verified by PCR by using P5', P3', and KanMX4 internal primers.

Plasmids—pMAC195 is a *URA3* centromeric plasmid that expresses a fully functional full-length yTaf_{II}19p from the *DED1* promoter. pMAC186 is a pUCBM21 derivative carrying the *TAF19* ORF cloned in the vector *EcoRV-SacI* sites. pML25 is a derivative of the pPC86 plasmid (24) containing the *TAF19* ORF cloned between the promoter and 3' untranslated sequences of *ADC1*. pMAC197 is a pET15b derivative carrying the *TAF19* sequences. It was created by the cloning of the *EcoRV-BamHI* fragment of pMAC186 into pET15b. The *TAF19* sequences of pML25 were replaced with the *taf19-1*, *taf19-7*, and *taf19-9* mutant sequences, leading to pML64, pML65, and pML66. pML98 is a pLex202 derivative (25) that encodes the LexA-yTaf_{II}19p fusion protein from the *ADC1* promoter. pML135, pML132, and pML133 are the same fusion to the mutant yTaf_{II}19p proteins. pML69, pML70, and pML71 are pPC62 (24) derivatives expressing yTaf_{II}19p, yTaf_{II}19-1p, and yTaf_{II}19-9p from the *ADC1* promoter. pML63 carries a GST-*TAF19* fusion cloned under the control of the arabinose-inducible *E. coli* *AraC* promoter. pML136 was generated by cloning a *Xba-HindIII* fragment encoding a tagged version of yTaf_{II}40p from pRS415-*TAF40* (26) into pRS424.

pMAC253 is a pET15b derivative that carries a 1.6-kilobase pair *HindIII-BamHI* fragment of *CCR4*, starting 472 nucleotides downstream of the ATG, thus expressing a truncated protein.

pMPM272 encodes GST from the arabinose-inducible *E. coli* *AraC* promoter (kindly provided by Mathias Mayer).

pU61 is a pET22b/pET15b derivative encoding a His₆-Not5 fusion protein (the fusion is at the N terminus of Not5p). A stop codon and 3' untranslated *NOT5* sequences separate the *NOT5* ORF and the pET22b His₆ sequences. Plasmids are summarized in Table II.

Cloning details are available upon request.

Isolation of *taf19* Mutant Alleles—pMAC186 was used as DNA template for *TAF19* PCR mutagenesis by using the classical forward and reverse primers and the *Taq* polymerase (Life Technologies, Inc.). PCR products were pooled and cloned in pML25 to replace the *TAF19* wild type allele. We obtained a library of 11×10^3 independent transformants that was transformed into MLY187.

Analysis of Transcript and Proteins Levels in *TAF19* and *taf19-1* Strains—After dilution from an overnight culture in rich medium, wild type and mutant cells were grown in rich medium to an A_{600} of 0.3 at 30 °C. The cultures were then shifted to 37 °C. At each time point indicated thereafter, total cellular RNA from the equivalent of $10 A_{600}$ of cells was extracted and analyzed by S1 nuclease protection assay as previously published (18, 27). The oligonucleotide for *NOT5* mRNA analysis was 5'-GCG AGG CTG ATT CTA CAC CTG GCG CGA TTG

GAG TCG TCG CCC TGT CTG ATA TAG AAA CAT CCC AAC AAC AA-3'. In parallel, equal amounts of cells (equivalent to 1 unit of A_{600}) were harvested by rapid centrifugation and washed with cold water, and total proteins were extracted according to Ref. 28. For this procedure, the frozen cell pellet was thawed on ice in 150 μ l of lysis buffer (1.85 M NaOH, 7.4% β -mercaptoethanol), vortexed, and left 10 min on ice. Proteins were then trichloroacetic acid-precipitated by the addition of 150 μ l of trichloroacetic acid 50% and resuspended in 80 μ l of SDS-PAGE sample buffer (40 μ l of 0.1 M NaOH and 40 μ l of 2 \times sample buffer). Equal amounts of total cell extracts (10 μ l) were then fractionated by SDS-PAGE and analyzed by Western blot using chemiluminescence (Pierce). Antibodies against yTaf_{II}s and TBP were kindly provided by Joe Reese and Anthony Weil. Antibodies against Not1p and Not5p were described previously (16, 21). Antibodies against yTaf_{II}19p and Ccr4p were raised. Briefly, recombinant yTaf_{II}19p was expressed from pMAC197, and recombinant Ccr4p was expressed from pMAC253, in BL21. The recombinant proteins were purified according to standard protocols (Qiagen) and were injected into rabbits (Elevage Scientifique des Dombes). Antibodies to yTaf_{II}19p were used at 1:3000, and those to Ccr4p were used at 1:8000.

Two-hybrid Interactions—To test protein-protein interactions, pLex202 derivatives were cotransformed into EGY48 (25) with pJG4-5 derivatives encoding galactose-inducible B42 fusions to Not proteins (16, 18), as well as to Ccr4p and Caf1p (19). Protein-protein interactions were scored as function of growth on synthetic galactose but not glucose minimal medium lacking leucine.

β -Galactosidase Assays—Strains carrying the fusion proteins to be tested were grown overnight in 1 ml of glucose minimal medium supplemented with leucine. The cells were washed twice in water and resuspended in 10 ml of galactose minimal medium supplemented with leucine. After 24 h, the cultures were collected, and β -galactosidase assays performed as described previously (17).

GST Pull-down Analysis—Unless otherwise stated, protein manipulations were performed at 4 °C. *E. coli* BL21(DE3) was transformed either with pMPM272 (encoding GST), pML63 (encoding GST-yTaf_{II}19p), or pU61 (encoding His₆-Not5p). Transformed cells were grown at 30 °C to an A_{600} of 0.6 in 100 ml of rich medium containing ampicillin (100 μ g/ml), and recombinant proteins were induced by addition of arabinose (final concentration, 0.5% in the case of GST and GST-yTaf_{II}19p) or isopropyl-1-thio- β -D-galactopyranoside (final concentration, 0.5 mM for His₆-Not5p). Cells were allowed to grow at 37 °C for 4 h, harvested, washed with cold water, resuspended in 5 ml of Buffer A (50 mM Tris-HCl, pH 7.5, 150 mM NaCl, 1 mM β -mercaptoethanol, 1 mM phenylmethylsulfonyl fluoride) supplemented with RNase A and DNase I (0.1 mg/ml, Sigma), and broken by sonication. Cellular debris and aggregates were discarded by centrifugation (20 min at 40,000 \times g), and supernatants were supplemented with glycerol (final concentration, 10%) and kept frozen until used. Equal total protein amounts (200 μ g) of His₆-Not5p extract were mixed with GST extract, GST-yTaf_{II}19p extract, or Buffer A, and the volume was brought to 100 μ l with Buffer A and Tween 20 (final concentration, 0.1%), making Buffer B. The concentration of His₆-Not5p and GST-yTaf_{II}19p in these extracts was roughly similar, with perhaps a 3-fold higher level of the former, as

determined by Coomassie staining. Tubes were incubated at 30 °C for 2 h. Reactions were centrifuged for 20 min at 40,000 × *g*, and 25 μl of a 50% gel slurry of glutathione-Sepharose beads (Amersham Pharmacia Biotech), previously equilibrated with Buffer B, was added to each supernatant. Suspensions were incubated at 30 °C for 1 h with a mild agitation and then centrifuged at 2000 × *g* for 1 min. Supernatant was kept on ice (fraction S), and beads were washed three times with 100 μl of cold Buffer B. The third wash was kept on ice (fraction W), and beads were resuspended with 100 μl of SDS-PAGE loading buffer (fraction B). Equal amounts (10 μl) of fractions S, W, and B were analyzed by Western blotting using antibodies directed against Not5p.

Yeast Extract Preparation—For preparation of total cell extracts 12 liters of cells grown to an A_{600} of 4.5 were pelleted and washed, and the pellet was frozen at –80 °C. This pellet was then slowly thawed and resuspended in 100 ml of lysis buffer (29), including 1 mM dithiothreitol and protease inhibitors. We additionally added a tip of DNase I (Sigma). Cells were broken in the cold with a French press (SLM AMINCO 20K Cell FA-073) three times at 1500 p.s.i. Then, the suspension was clarified first by 20 min at 16,000 × *g* and 1 h at 35000 rpm in a Beckman Ti35 ultracentrifuge.

For fractionation by ammonium sulfate precipitation, first 109 g/liter were added to the extract resulting in 30% ammonium sulfate. The precipitate was removed by ultracentrifugation (1 h centrifugation at 35,000 rpm in a Ti35 rotor) and 86 g/liter were then added to the supernatant leading to a 45% ammonium sulfate solution. The precipitate was collected by the same ultracentrifugation procedure, and 59 g/liter were added to the supernatant leading to 55% ammonium sulfate concentration. Finally, after collecting the precipitate the same way, 93 g/liter were added to the supernatant, leading to 70% ammonium sulfate. The pellets were resuspended in the minimal amount of lysis buffer carrying additionally 0.1% Nonidet P-40 and then dialyzed against 100 volumes of the same buffer. 300 μl of the dialyzed 45% cut of the cell extract was then analyzed by gel filtration (see below).

Gel Filtration Analysis—For gel filtration analysis, 300 μl of total cell extracts were loaded on a Superose 6 gel filtration column equilibrated with 350 mM NaCl, 10% glycerol, 0.1% Tween 20, and 40 mM Hepes, pH 7.3. The column was run at 0.4 ml/min, and 400 μl fractions were collected starting at 16 min and analyzed by Western blot analysis for the presence of yTaf_{II}19p (10–15% Tris Tricine gel). The position of the void volume was determined by the elution of salmon sperm DNA.

RESULTS

Isolation of Conditional Alleles of TAF19—We have suggested that the Ccr4-Not complex regulates transcription by sequestering or inhibiting transcription factors more specifically required for TBP function at TATA-less promoters. A potential candidate for such a factor is yTaf_{II}19p. To start investigating whether yTaf_{II}19p is associated with Ccr4-Not function, we used a genetic approach and first created a library of mutant *TAF19* alleles. *TAF19* was mutagenized by error-prone PCR amplification of *TAF19*, and the library of mutant alleles was cloned into a yeast *TRP1* centromeric plasmid (pML25). This library was transformed into MLY187, a yeast strain carrying a complete disruption of the genomic *TAF19* gene complemented by pMAC195, a *URA3* centromeric plasmid carrying a wild type copy of *TAF19*. Transformants were streaked on 5-fluoroorotic acid to select for the loss of the episomal wild type copy of the *TAF19* gene. The 5-fluoroorotic acid-resistant transformants were streaked on rich medium at 16, 30 and 37 °C to determine whether conditional mutants had been isolated.

Out of this screen, we further characterized three *taf19* mutants, called 19-1, 19-7, and 19-9. *taf19-7* grew slowly on rich medium and at all temperatures, whereas the other two mutants grew well on rich medium at 30 °C but were temperature-sensitive (Fig. 1A). These phenotypes were recessive. The mutant alleles were sequenced. *taf19-1* carries four mutations that result in four amino acid changes (D46G, L63H, L79D, and K98M), *taf19-9* also carries four mutations that result in four amino acid changes (D24G, E38G, N57D, and F70S), and finally, *taf19-7* is a point mutant that results in a single amino acid change (K13E). Fig. 1B shows the position of these mutations within the yTaf_{II}19p.

Because *taf19-1* and *taf19-9* carry multiple mutations, we tried to determine whether any individual mutation was responsible for the temperature-sensitive phenotype. Many of these mutations lie in the domain of yTaf_{II}19p that is thought to be involved in dimerization with yTaf_{II}40p (15). Particularly, residue Asp-24 is conserved between yTaf_{II}19p and orthologs from human, *Drosophila*, and *Caenorhabditis elegans*. In the three-dimensional structure (huTaf_{II}18-huTaf_{II}28 heterodimer structure), the huTaf_{II}18p Asp-45 residue (corresponding to yTaf_{II}19p Asp-24) is involved in a strong hydrogen bond network that stabilizes the heterodimer. On the other hand, this heterodimer is also stabilized by multiple hydrophobic interactions occurring at the crossover of two α-helices (in huTaf_{II}18p, residues 60–70 of the α2-helix). A mutation lying in this area (yTaf_{II}19p Asp-46 corresponds to huTaf_{II}18p Glu-67) might induce a local disorganization of the α2-helix, resulting in the destabilization of the heterodimer. Surprisingly, in the case of *taf19-1*, neither D46G alone nor an allele carrying the other three mutations (L63H, L79D, and K98M) conferred a temperature-sensitive phenotype (data not shown). Thus, temperature sensitivity is conferred by D46G and at least one other mutation. Similarly, in the case of *taf19-9*, D24G alone does not confer temperature sensitivity. However, temperature sensitivity might still result from a disruption of this dimerization domain, which in turn might require more than one mutation. This hypothesis was confirmed by the fact that overexpressing *TAF40* (from plasmid pML136) suppressed the temperature sensitivity of *taf19-1* and *taf19-9* (MY2268–MY2271; see Table I) at 36 °C (data not shown). In this context, it is interesting to note that temperature-sensitive *taf40* alleles were also found to carry multiple mutations within the equivalent yTaf_{II}40p dimerization domain and that this temperature-sensitive phenotype was also alleviated by overexpressing yTaf_{II}19 (14).

Phenotypic Analysis of the taf19-1 and taf19-9 Mutants—Not much is known about *TAF19*. We thus first further characterized the two conditional alleles that we had isolated, namely *taf19-1* and *taf19-9*. Fig. 1C shows that both mutants rapidly arrest cell growth as the cells are shifted to the restrictive temperature. Viability of the *taf19* mutants was assayed at given times after the temperature shift and was found to be very weakly affected only after 6 h at the restrictive temperature (data not shown).

Our interest in isolating *taf19* mutant alleles was based upon a previous description of the preferential loss of transcription from TATA-less promoters upon yTaf_{II}19p depletion (12). However, similar results were described with yTaf_{II}40p, yet, as mentioned above, more recently, yTaf_{II}40p has been said to be generally required for transcription (14). To determine what phenotype our conditional mutants displayed at restrictive temperature upon loss of yTaf_{II}19p function, total cellular RNA was extracted from wild type and *taf19-1* cells just prior to the shift to the restrictive temperature and at given times after the shift. This RNA was analyzed by S1 mapping first for the levels of the *DED1* transcript expressed from a TATA-containing promoter, and the *NOT5* and *HIS4* transcripts that do not depend upon a canonical TATA sequence. It should be clarified that we claim that *NOT5* has no canonical TATA based on the sequence of the promoter region. In the case of *HIS4*, this has been previously reported (30). In *taf19-1* cells, within 4 h after the shift, the levels of the *HIS4* and *NOT5* transcripts decreased to a nondetectable level, whereas the level of the *DED1* transcript remained stable (Fig. 2A). At later time points (6 h), the *DED1* transcript also decreased (data not shown). Because the *HIS4* and *DED1* transcripts have been described to have similar half-lives (27), this result suggests that *HIS4* transcrip-

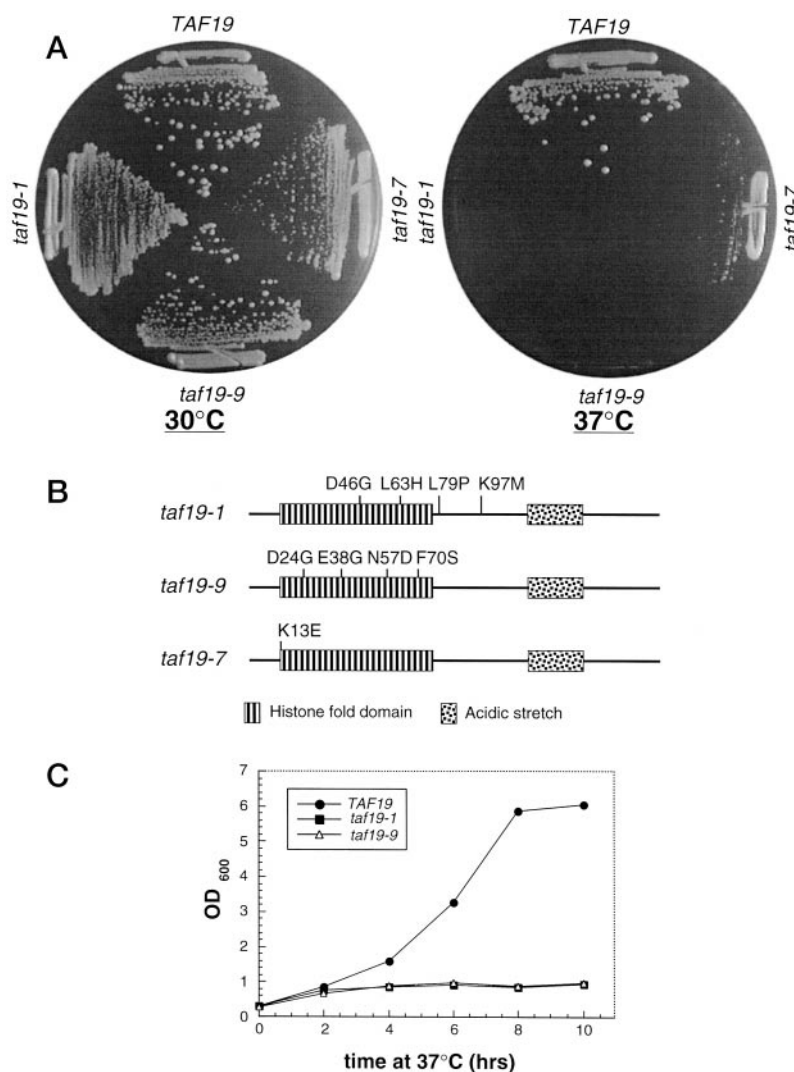


FIG. 1. Characterization of *taf19* mutant alleles. **A**, growth of wild type and mutant *taf19* strains. Two temperature-sensitive mutants (*taf19-1* and *taf19-9*) and one sick mutant (*taf19-7*) were isolated and streaked together with the isogenic wild type *TAF19* strain on YPD plates at 30 and 37 °C as indicated. Strains used were MLY268 (*TAF19*), MLY270 (*taf19-1*), MLY272 (*taf19-7*), and MLY274 (*taf19-9*). **B**, schematic structure of yTaf_{II}19p with the position of amino acid substitutions in the mutant yTaf_{II}19 proteins. This scheme is based on the alignment in Ref. 15. **C**, growth curve of wild type or *taf19* mutants at 37 °C. MLY268, MLY270, and MLY274 were grown in YPD at 30 °C to an A₆₀₀ of 0.3, and the cultures were then shifted to 37 °C. In parallel, cultures that were kept at 30 °C grew similarly, independently of the *TAF19* allele (data not shown).

tion is more rapidly affected than *DED1* transcription. Because we realized that the *taf19* mutants isolated grew slowly on minimal medium lacking threonine or isoleucine, we also investigated the *ILV1* transcript levels in wild type and mutant cells shifted to the restrictive temperature for 4 h, because the *ILV1* gene lies in the pathway of the biosynthesis of both amino acids. This mRNA has been reported to be transcribed from a TATA-less promoter (31), and it was also dramatically decreased 2 h after the shift to the restrictive temperature (Fig. 2B). We then similarly analyzed the levels of an unstable tRNA (27) and found that transcription by RNA polymerase III was not measurably affected in either strain (Fig. 2B). Finally, we looked at *HIS3* transcript levels and found that whereas transcription of *HIS3* from both promoters decreased upon inactivation of yTaf_{II}19p, that from the TATA-less promoter decreased more rapidly and more severely (Fig. 2C, compare lane 4 to lane 1). Taken together these results suggest that the loss of yTaf_{II}19p function affects more rapidly transcription from the TATA-less promoters (*HIS3*, *HIS4*, *NOT5*, and *ILV1*) than from the canonical TATA-containing promoters (*HIS3* and *DED1*).

Decreased Steady State Level of TFIID Components upon yTaf_{II}19p Inactivation—It has not been demonstrated that yTaf_{II}19p is definitively part of TFIID. It is thought to be, by homology with its human counterpart (15) and because it co-immunoprecipitates with both yTaf_{II}145p and TBP (12). Because it has been reported that depletion of given yTaf_{II}s leads

to degradation of other yTaf_{II}s that are part of the same complex, we investigated whether inactivation of yTaf_{II}19p similarly affected the steady state levels of other yTaf_{II}s. Total protein extracts were prepared in parallel to the RNA mentioned above, and they were analyzed by Western blot for the levels of different yTaf_{II}s. As shown on Fig. 3, in *taf19-1* mutant cells, the levels of specific TFIID yTaf_{II}s (yTaf_{II}145p and yTaf_{II}40p) rapidly decreased upon inactivation of yTaf_{II}19p. The levels of other yTaf_{II}s, shared between the TFIID and SAGA complexes, such as yTaf_{II}60p, yTaf_{II}68p, and yTaf_{II}90p, or even with the SWI/SNF complex, such as yTaf_{II}30p, decreased somewhat slower or were unaltered after 4 h at the restrictive temperature. TBP levels decreased rapidly to a lower stable level. The levels of yTaf_{II}19p itself were undetectable in up to 100 μg of total cell extract with the antibodies that we raised.

These results are very similar to what has been described previously for temperature-sensitive *taf40* mutants (14) and support the presence of yTaf_{II}19p in TFIID. They also suggest that the inactivation of yTaf_{II}19p leads to the destabilization of TFIID through the degradation of some specific TFIID Taf_{II}s (e.g. yTaf_{II}40p and yTaf_{II}145p). Moreover, yTaf_{II}25p, a yTaf_{II} shared by TFIID and SAGA, was rapidly decreased upon yTaf_{II}19p inactivation. In that context, it is interesting to note that upon yTaf_{II}25p inactivation, yTaf_{II}19p was also rapidly degraded (32).

We also investigated the levels of some of the components of

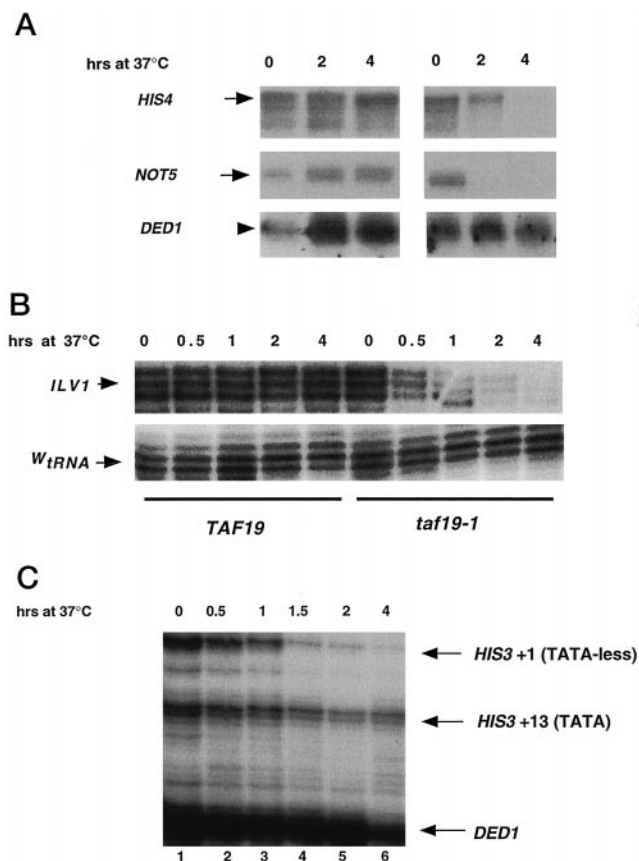


FIG. 2. TAF19 may generally affect transcription, but it is preferentially required for transcription from TATA-less promoters. A, MLY268 and MLY270 were grown in YPD at 30 °C to an A_{600} of 0.3, and cultures were then shifted to 37 °C. Total RNA was extracted from *TAF19* and *taf19-1* strains at the indicated time points after shifting to 37 °C. 50 μ g of total RNA were analyzed by S1 nuclease protection assay for the levels of the indicated transcripts. Transcription of *HIS4* depends upon a TATA-less core promoter in *gcn4 Δ* strains (30), and sequence analysis shows that the *NOT5* promoter does not contain a canonical TATA sequence. In contrast the *DED1* promoter carries a canonical TATA sequence. The hybridizations were internally controlled by simultaneous hybridization of *NOT5* and *HIS4* with *DED1*. Similar results were obtained with the *taf19-9* temperature-sensitive mutant (data not shown). B, the same experiment was performed, and the total cellular RNA was hybridized to measure the levels of *ILV1* and *WtRNA*. The *ILV1* is also thought to carry a TATA-less promoter. C, the same experiment was performed with strain MLY270 alone, and total cellular RNA was hybridized to measure the levels of the *HIS3* and *DED1* transcripts.

the Ccr4-Not complex. All of the components that were analyzed, namely Not1p, Not5p, and Ccr4p, also decreased, but not as dramatically, nor as quickly, as the yTaf_{II}s. Because, at least in the case of *NOT5*, we have found that transcription is affected by the loss of yTaf_{II}19p, the decrease in Not5p may be a consequence of protein turnover. In any event, it is important to note that the levels of the different Ccr4-Not components were similar in the wild type and mutant strains at the permissive temperature.

taf19 Mutants Display Synthetic Phenotypes with Specific not Mutants—We next used a genetic approach to determine whether the function of yTaf_{II}19p was related to that of the Ccr4-Not complex. We constructed a large number of double mutants by crossing *taf19-1* and *taf19-9* to many *ccr4-not* mutants, sporulating diploids and dissecting tetrads. The phenotypes of the double mutants were compared with the phenotypes of the single mutants to look for synthetic lethal interactions or suppression. In particular, growth on rich medium at 16, 30, and 37 °C as well as growth on minimal medium at

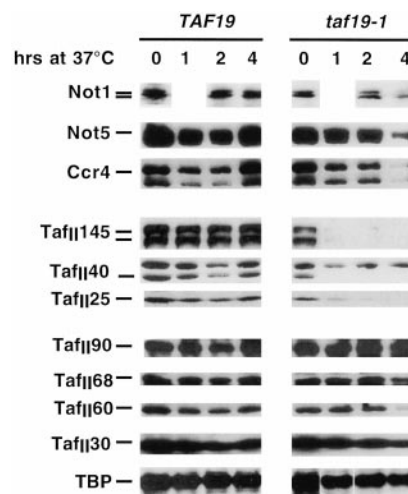


FIG. 3. Decreased steady state levels of yTaf_{II}s, TBP, and Ccr4-Not complex subunits upon inactivation of TAF19. MLY268 (*TAF19*) and MLY270 (*taf19-1*) were grown in YPD at 30 °C to an A_{600} of 0.3, and cultures were then shifted to 37 °C. At different time points (as indicated) after the shift at 37 °C, total proteins were extracted from equal amounts of cells (see under “Experimental Procedures”). Protein extracts from equal amounts of cells were then fractionated by SDS-PAGE and blotted to nitrocellulose. The levels of different TFIID and Ccr4-Not complex subunits (as indicated) were analyzed by Western blot.

permissive temperature was analyzed. *not1-1*, *not1-2*, *not2-1*, *not2-4*, *not3::URA3*, *caf1::LEU2*, and *ccr4::URA3* mutants did not show any obvious genetic interaction with *taf19-1* or *taf19-9*. In contrast, *not4* and *not5* mutants did. *not4-1*, but more dramatically *not4::LEU2*, showed a synthetic phenotype when combined with both *taf19-1* and *taf19-9* on minimal medium at 30 °C (Fig. 4). This same effect was observed when the minimal medium was complemented with histidine (data not shown). A slight synthetic growth phenotype could also be detected on rich medium at 30 °C (not shown). More interestingly, *not5::LEU2* and *not5-1*, but not *not5-2*, displayed a dramatic synthetic growth phenotype on minimal medium when combined with either one of the two *taf19* mutants (Fig. 4). The two alleles, *not5-1* and *not5-2*, are similar in that they both carry nonsense mutations (16), but they can be distinguished by the fact that the protein encoded by *not5-1* is shorter (see Fig. 4, bottom). Such an allele-specific synthetic phenotype strongly supports the fact that yTaf_{II}19p and Not5p functionally interact for growth on minimal medium and may even be physically associated. Alternatively, yTaf_{II}19p and the Ccr4-Not complex may participate independently in transcriptional regulation required for growth on minimal medium, and the contribution of the Ccr4-Not complex may be only seriously impaired when Not4p is absent or when Not5p is sufficiently truncated.

TAF19 Interacts by Two-hybrid with NOT5—To investigate further whether or not yTaf_{II}19p and Not5p may interact, we performed a two-hybrid analysis. A plasmid expressing a LexA-yTaf_{II}19 fusion protein was constructed (pML98, see under “Experimental Procedures”) and found to complement a null mutation of *TAF19*. It was transformed into a strain carrying a *leu2* gene under the control of LexA operators (EGY48; see Table I). Additional plasmids were co-transformed that expressed fusions of all the known components of the Ccr4-Not complex to the B42-activation domain (16, 18) under the control of the *GAL1* promoter. Growth on glucose or galactose plates devoid of leucine was investigated. Fig. 5 shows that a positive two-hybrid interaction could be detected among *TAF19* and *NOT5*, *NOT3*, *NOT2*, and *CAF1* (the latter two to a lesser

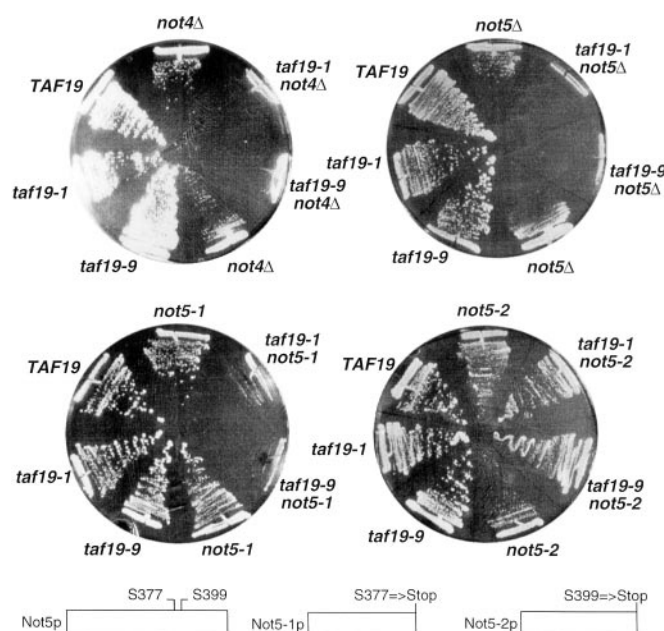


FIG. 4. Synthetic slow growth of double *taf19* and *not4* or *not5* mutants on minimal medium. Double mutants, isogenic single mutants and wild type strains were streaked together on minimal plates lacking histidine at 30 °C. Strains used were MLY268 (*TAF19*), MLY270 (*taf19-1*), MLY274 (*taf19-9*), YOU584 (*not4Δ*), MLY365 (*not4Δ taf19Δ + TAF19*), MLY367 (*not4Δ taf19Δ + taf19-1*), MLY369 (*not4Δ taf19Δ + taf19-9*), MY1719 (*not5Δ*), MLY329 (*not5Δ taf19Δ + TAF19*), MLY331 (*not5Δ taf19Δ + taf19-1*), MLY333 (*not5Δ taf19Δ + taf19-9*), YOU123 (*not5-1*), MLY347 (*not5-1 taf19Δ + TAF19*), MLY349 (*not5-1 taf19Δ + taf19-1*), MLY351 (*not5-1 taf19Δ + taf19-9*), YOU142 (*not5-2*), MLY353 (*not5-2 taf19Δ + TAF19*), MLY355 (*not5-2 taf19Δ + taf19-1*), and MLY357 (*not5-2 taf19Δ + taf19-9*). At the bottom of the figure are shown schemes of the Not5 wild type and mutant proteins. The growth of the various strains was no different when the plates were supplemented with histidine (data not shown).

extent). Growth of all of these strains on galactose minimal medium supplemented with leucine was compared and found to be indistinguishable, except that the strains carrying *B42-NOT2* and *B42-NOT3* grew somewhat more slowly (data not shown). To confirm these results, the expression of β -galactosidase was measured in the same strains after growth for 24 h in liquid galactose minimal medium supplemented with leucine. Table III summarizes these results. With this second reporter, an interaction between yTaf_{II}19p and Not2p, Not3p, and Not5p is confirmed, and an interaction between yTaf_{II}19p and Ccr4p is additionally detectable. No interaction can be measured between yTaf_{II}19p and Caf1p with this second reporter. Finally, no interaction between Not1p or Not4p and yTaf_{II}19p was detectable with either of the two reporters. These results support the existence of a physical interaction between yTaf_{II}19p and components of the Ccr4-Not complex, in particular Not5p, that was suggested by the allele-specific synthetic growth phenotypes presented above.

One way to investigate further whether the interaction between yTaf_{II}19p and Not5p is functionally relevant is to determine whether any of the *taf19* mutants isolated are defective in this interaction. We thus introduced the *taf19* mutations into the construct expressing LexA-yTaf_{II}19p (pML132, pML133, and pML135; see under "Experimental Procedures"). Except for LexA-yTaf_{II}19-7p, all new fusion proteins complemented the null mutation of *TAF19* and were expressed at the same level as LexA-yTaf_{II}19 (data not shown). The new fusions were tested for a two-hybrid interaction with B42-Not5p (see Fig. 5, bottom panel). No interaction was detected between LexA-yTaf_{II}19-1p and B42-Not5p, whereas in contrast, the LexA-yTaf_{II}19-9 protein interacted with B42-Not5p, in a man-

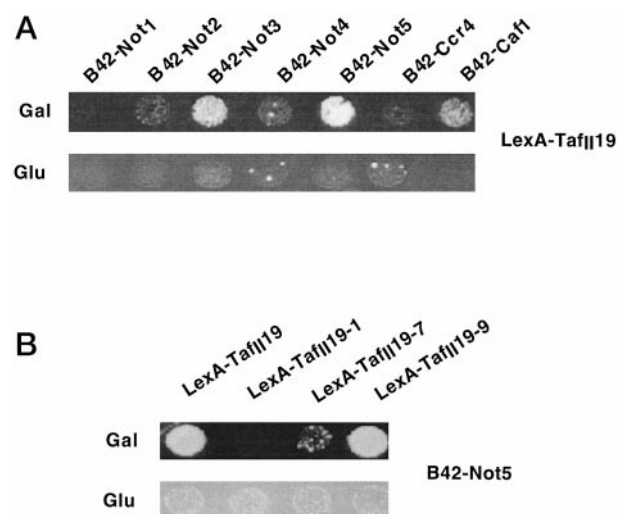


FIG. 5. TAF19 interacts with NOT5 in the two-hybrid assay. A, EGY48 was transformed with pML98 (LexA-yTaf_{II}19p) together with pJG4-5 derivatives expressing either the B42-Not1, B42-Not2, B42-Not3, B42-Not4, B42-Not5, B42-Ccr4, or B42-Caf1 fusion proteins as indicated. B, EGY48 was transformed with the plasmid expressing the B42-Not5 fusion protein, together with plasmids encoding fusion proteins of LexA to either wild type or mutant forms of yTaf_{II}19p as indicated. In both cases, transformants were grown overnight in synthetic glucose medium supplemented with leucine. Cells were harvested, washed twice in cold water, and allowed to grow for 4 h in synthetic galactose medium supplemented with leucine. Equal amounts of cell culture (1 A₆₀₀ unit) were washed with water, serially diluted, and spotted either on YPD, glucose minimal medium (*Glu*), or galactose minimal medium (*Gal*). The same strains were streaked on galactose minimal medium supplemented with leucine and grew indistinguishably, except the strains expressing B42-Not2p and B42-Not3p that grew somewhat slower (data not shown).

TABLE III

β -Galactosidase assays to measure two-hybrid interactions

The indicated strains are described in Table I, and all carry the LexA-*LacZ* reporter gene. All of these strains carry LexA-Taf_{II}19p and the indicated B42 fusion protein. The values for β -galactosidase activity indicated for two separate experiments were calculated in nmol \times mg⁻¹ min⁻¹.

Strain name	B42 Fusion protein	Experiment 1	Experiment 2
MLY637	B42	8.5	7.9
MLY638	B42-Not1p	5.5	4.6
MLY639	B42-Not2p	31.1	19.8
MLY640	B42-Not3p	27.2	26.2
MLY641	B42-Not4p	5.2	6.8
MLY642	B42-Not5p	35.5	34.9
MLY643	B42-Ccr4p	34.8	34.7
MLY644	B42-Caf1p	5.8	5.8

ner indistinguishable from LexA-yTaf_{II}19p. Thus, not all *taf19* mutants isolated are detectably defective in yTaf_{II}19p-Not5p interaction, but the finding that one is, is additional support for a functional physical association of yTaf_{II}19p and Not5p *in vivo*. Indeed, yTaf_{II}19-1p and LexA-yTaf_{II}19-1p are functional at the permissive temperature, because they replace a wild type yTaf_{II}19p for vegetative growth. This indicates that the proteins are correctly folded. Hence, the absence of interaction with Not5p indicates that mutated residues in yTaf_{II}19-1p are important for interaction with Not5p.

yTaf_{II}19p and Not5p Associate Physically in Vitro—Because the two-hybrid experiments described above are performed *in vivo*, they do not define whether or not yTaf_{II}19p and Not5p can interact directly. To address such a question, we prepared bacterial extracts from *E. coli* expressing GST-yTaf_{II}19p, GST alone, or His₆-Not5p recombinant proteins to test their interaction *in vitro*. The expression and solubility of all proteins was verified by analyzing the total soluble bacterial extracts by

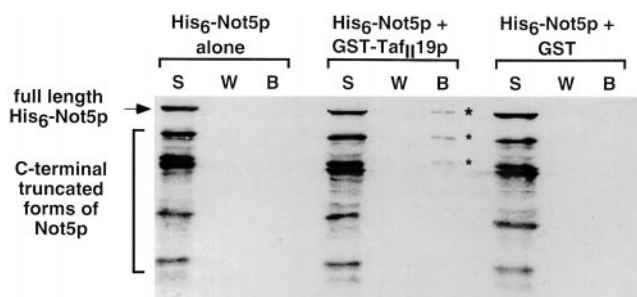


FIG. 6. yTaf_{II}19p interacts directly with Not5p *in vitro*. Bacterial extracts containing His₆-Not5p were mixed with bacterial extracts devoid of any recombinant protein (*left three lanes*), with bacterial extracts containing recombinant GST-yTaf_{II}19p (*middle three lanes*), or with bacterial extracts containing recombinant GST alone (*right three lanes*). After 2 h at 30 °C, the reactions were incubated with glutathione-Sepharose beads. Equivalent amounts of unbound fraction (S), the third bead wash (W), and the bound fraction (B) were analyzed by SDS-PAGE followed by Western blot analysis with antibodies to Not5p. The major visible forms of His₆-Not5p were all capable of binding Ni-nitrilotriacetic acid agarose, suggesting that they are C-terminal Not5p truncations. Only the largest forms were found in fraction B, specifically in the case of incubation with recombinant GST-yTaf_{II}19p, and are labeled with an *asterisk*. The same results were obtained when binding was performed with 300 mM salt and 0.5% Tween 20 and were reproduced many times.

Western blotting with antibodies to the GST moiety or to Not5p (data not shown). Not5p was detected as multiple forms (as can be seen in S lanes of Fig. 6), most likely resulting from protein degradation. Most of these detectable forms were capable of binding Ni-nitrilotriacetic acid agarose (data not shown), suggesting that they were stable C-terminal truncations.

Bacterial extracts containing His₆-Not5p were incubated with Buffer A or with bacterial extracts containing either GST or GST-yTaf_{II}19p in the presence of 150 mM salt and 0.1% Tween 20 (see under "Experimental Procedures"), and glutathione-Sepharose beads were then added. The beads were washed, and then the unbound extract (Fig. 6, S), wash (W), and beads (B) were analyzed by Western blot for the presence of Not5p. His₆-Not5p was retained on the beads specifically in the presence of GST-yTaf_{II}19p. Interestingly, only the three longest forms of His₆-Not5p (all capable of binding Ni-nitrilotriacetic acid agarose) were retained on the beads carrying GST-yTaf_{II}19p. Similar results were obtained with higher stringency (300 mM salt and 0.5% Tween 20) (data not shown). These results demonstrate that yTaf_{II}19p and Not5p can directly associate in the absence of other yeast proteins. It appears that the interaction between yTaf_{II}19p and Not5p requires a minimal N-terminal Not5p fragment, a finding that might relate directly to the observation that the *not5-1* allele, but not the *not5-2* allele, which encodes a longer protein, displays synthetic growth phenotypes with *taf19* mutants *in vivo*.

yTaf_{II}19p Is Found in Multiple Complexes *in Vivo*—The results presented so far demonstrate allele- and gene-specific genetic interactions between *TAF19* and genes encoding components of the Ccr4-Not complex. They further show that yTaf_{II}19p and Not5p physically interact. These results are in agreement with a model whereby components of the Ccr4-Not complex might be associated with and regulate yTaf_{II}19p. Our findings also confirm the hypothesis that yTaf_{II}19p is part of the TFIID complex, but it is not known whether it may be part of any other complexes, such as Ccr4-Not complexes. As mentioned above, with the antibodies that we raised, we could not detect yTaf_{II}19p in 100 μg of total cell extracts by Western blot analysis. However, we could detect yTaf_{II}19p very specifically in 45 and 55% ammonium sulfate cuts of total cell extracts (Fig. 7A). In contrast to this very specific fractionation of yTaf_{II}19p, yTaf_{II}145p (and other yTaf_{II}s) fractionated with a

very broad profile, from the 30% ammonium sulfate cut to the supernatant of the 70% ammonium sulfate cut (Fig. 7A). This material enriched for yTaf_{II}19p was analyzed by Superose 6 gel filtration to determine whether yTaf_{II}19p was associated in complexes other than TFIID. Fig. 7B shows that the majority of yTaf_{II}19p is associated in very large complexes. Fractionation by Sepharose 4B allowed us to clearly define that these yTaf_{II}19p complexes of a size apparently greater than 1 MDa were soluble complexes and not aggregated proteins (data not shown). When equal protein amounts of each fraction were loaded on the gel rather than equal volume equivalents of each fraction, small amounts of yTaf_{II}19p were also detectable as eluting with a very broad profile, as has been previously shown for yTaf_{II}145p (33) (Fig. 7C). This shows that yTaf_{II}19p also appears to elute in fractions 18, 22, and 26.

DISCUSSION

yTaf_{II}19p is one of the less well characterized yTaf_{II}s so far. It is the homologue of human Taf_{II}18p, which is known to be part of the human TFIID complex and to form dimers with human Taf_{II}28p according to a histone-fold type of structure (15). In yeast, *TAF19* is essential for vegetative growth, and one report has demonstrated that not all transcription decreases similarly upon yTaf_{II}19p depletion but that transcription from TATA-less promoters is preferentially arrested (12). The same was reported for the yeast homologue of human Taf_{II}28p, namely yTaf_{II}40p (13), but a recent study claims that in fact yTaf_{II}40p is generally required for RNA polymerase II transcription (14). In the latter, Komarnitsky *et al.* show that the temperature-sensitive phenotype of the *taf40* alleles isolated could be suppressed by overexpression of yTaf_{II}19p, suggesting that yTaf_{II}19p should also be generally required for transcription. We have isolated temperature-sensitive *taf19* alleles. By analyzing the levels of transcripts of similar half lives (27), we found that not all transcription decreases with similar rapidity upon loss of yTaf_{II}19p function, supporting the selective requirement for yTaf_{II}19p function previously published (12). We did find that within 6 h of yTaf_{II}19p inactivation, all RNA polymerase II transcripts measured decreased. However, this general late effect could clearly be indirect, especially if one considers that yTaf_{II}19p is needed for the stability of one or more transcription complexes (*e.g.* TFIID). In fact, this late effect also correlates with the appearance of a drop in viability. All conditional alleles of *TAF19* that we isolated carry multiple mutations, similarly to the *taf40* temperature-sensitive alleles that were isolated (14). Most of these mutations also lie in the region of *TAF19* that encodes the domain of yTaf_{II}19p thought to interact with yTaf_{II}40p. Our analysis demonstrated that multiple mutations are necessary to confer a temperature-sensitive phenotype. This might suggest that multiple mutations are necessary to disrupt a yTaf_{II}19p-yTaf_{II}40p interaction. Alternatively, temperature sensitivity might require the loss of yTaf_{II}19p interaction with multiple proteins. Because overexpression of *TAF40* suppresses temperature sensitivity of the mutant *taf19* alleles, the former seems a more likely explanation.

By the two-hybrid assay and GST pull-down analysis, we have demonstrated that yTaf_{II}19p can interact with Not5p, both *in vitro* and *in vivo*. This interaction is direct and does not require any other yeast protein. Interestingly, one of the *taf19* mutants isolated, namely that encoding yTaf_{II}19-1p, was no longer able to interact with Not5p in the two-hybrid assay, even at 30 °C. At the permissive temperature and on rich media, the strain MLY270 (*taf19-1*) grew as well as the wild type, suggesting that the mutant protein is functional and has a global unaltered conformation. Hence, the fact that yTaf_{II}19-1p does not interact with Not5p indicates that one (or

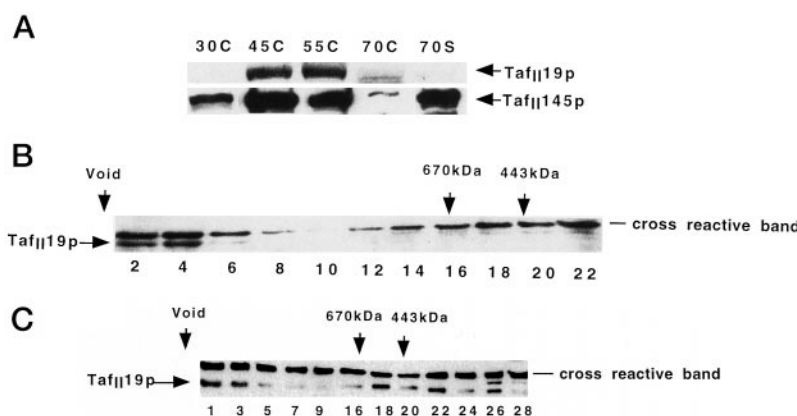


FIG. 7. **Most yTaf_{II}19p has a very restricted distribution to large protein complexes.** A, total protein extracts from wild type cells were incubated with 30% ammonium sulfate. The supernatant was brought to 45, 55, and finally 70% ammonium sulfate. The precipitates at each concentration were resuspended and dialyzed against the extract buffer, and 50 μ g of each fraction (lanes 30C, 45C, 55C, and 70C), as well as 50 μ g of the final supernatant (lane 70S), were analyzed by Western blot for the presence of yTaf_{II}19p and yTaf_{II}145p as indicated. B, 300 μ l of fraction 45C was analyzed by Superose 6 gel filtration. Every second fraction was analyzed by SDS-PAGE followed by Western blot analysis with antibodies against yTaf_{II}19p. The position of the void volume and marker proteins of known size are indicated at the top. The position of yTaf_{II}19p and a cross-reactive band are indicated. Similar results were obtained with fraction 55C. C, to reveal the possible presence of yTaf_{II}19p in fractions other than fractions 1–4, the protein concentration of each fraction was measured, and equivalent amounts were similarly analyzed by Western blot for the presence of yTaf_{II}19p. The fractions displayed on the figure are the only ones in which yTaf_{II}19p was reasonably detected (lane numbers correspond to fraction numbers). Fraction 18 corresponds to a size of 550 kDa, fraction 22 to 350 kDa, and fraction 26 to 228 kDa.

some, if not all) of the mutated residues is directly involved in this interaction and may define the yTaf_{II}19p domain interacting with Not5p. Within Not5p, we did not precisely localize the domain responsible for interaction with yTaf_{II}19p, but we could show that it was in the N terminus of the protein. In this most N-terminal part of Not5p, the first 207 amino acids are highly conserved in Not3p (40% identity), and we also detected a yTaf_{II}19p-Not3p interaction in our two-hybrid assay. Despite the fact that we did not try to confirm this interaction by GST pull-down analysis, it is tempting to suggest that this conserved domain might be the yTaf_{II}19p target. We are currently testing this hypothesis. The yTaf_{II}19p human homologue is quite well characterized, and complexes containing this Taf_{II} have been isolated (15). On the other hand, human homologues of the yeast genes encoding Ccr4-Not complex subunits have been isolated (34). Our study thus provides us with a tool to expand the comprehension of Taf_{II} function in the mammalian system, and it will be very interesting to determine whether the yTaf_{II}19p-Not5p interaction is also conserved in human.

Characterization of the level of components of the TFIID complex upon loss of yTaf_{II}19p function at the restrictive temperature demonstrates that, similarly to what has been reported for the depletion of other Taf_{II}s, the steady-state level of a number of Taf_{II}s specific to TFIID (yTaf_{II}40p and yTaf_{II}145p) decreases to undetectable levels very rapidly. The level of TBP also rapidly decreases to a lower level. In fact, we show that loss of yTaf_{II}19p has effects very similar to those of the depletion of yTaf_{II}40p, as described previously (14). Taken together with the fact that overexpression of *TAF40* suppresses the mutant *taf19* alleles that we isolated and with the fact that yTaf_{II}19p can coimmunoprecipitate with TBP and yTaf_{II}145p (12), these results support the idea that, like yTaf_{II}40p, yTaf_{II}19p is part of TFIID. Further support comes from our finding that yTaf_{II}40p and yTaf_{II}145p, so far only described in TFIID and not in SAGA, co-purified with GST-yTaf_{II}19p (data not shown).

It is not known how many different yTaf_{II}19p-containing complexes may exist. We found that most of the yTaf_{II}19p from total cell extracts fractionates with a size greater than 1 MDa, as determined both by Superose 6 and Sepharose 4B gel filtration. One can also detect some yTaf_{II}19p in three separate peaks, one of which corresponds to a size that could be TFIID

(fraction 18). Although the steady-state level of some yTaf_{II}s (yTaf_{II}60p, yTaf_{II}68p, and yTaf_{II}90p) present in TFIID and SAGA remained relatively stable upon yTaf_{II}19p inactivation, that of yTaf_{II}25p (also found in both complexes) rapidly decreased. Conversely, yTaf_{II}19p disappears rapidly upon yTaf_{II}25p depletion (32). Thus, our results do not exclude the possible presence of yTaf_{II}19p in SAGA. In this regard, we have found that the *taf19* alleles that we isolated are synthetic lethal with the null allele of *SPT3* (data not shown). Spt3p contains histone-fold domains homologous to both those of yTaf_{II}19p and yTaf_{II}40p, and a model structure for Spt3p in which these two domains interact has been proposed (15). Nevertheless, one cannot exclude that yTaf_{II}19p interacts with the yTaf_{II}40-homologous histone-fold domain of Spt3p and thus may be present in the SAGA complex. This could account for the synthetic lethality mentioned above. Alternatively, yTaf_{II}19p is not in SAGA, and the *taf19-spt3* synthetic lethality could be explained by the combined impairment of TFIID and SAGA function (or of yet other Taf_{II}-containing complexes). Further studies will be needed to elucidate this ambiguity. Whether or not yTaf_{II}19p is in SAGA as well as in TFIID (and maybe in other complexes), it appears that the mutant phenotype of the alleles that we isolated can be suppressed by increasing yTaf_{II}40p levels. Thus, the interaction with the Ccr4-Not complex that is suggested by the genetic interactions that we described probably involves complexes that carry both yTaf_{II}19p and yTaf_{II}40p. This would argue in favor of TFIID or another complex, but not SAGA.

The question of whether yTaf_{II}19p is associated in large Ccr4-Not complexes or only interacts transiently with components of the complex will require more work. Our findings clearly demonstrate that yTaf_{II}19p can associate with Not5p directly, and interacts with at least four other components of the complex by the two hybrid assay. Surprisingly Not4p is not one of these, yet *not4* mutants display genetic interactions with the *taf19* mutants. However, we know that the absence of Not4p dramatically decreases the association of Not5p in large Ccr4-Not complexes.²

Our present results are consistent with there being a func-

² M. A. Collart, unpublished observations.

tional interaction between the Ccr4-Not complex and TFIID, as has been previously suggested. Indeed, one can imagine that there is an equilibrium between the different *yTaf_{II}19p* and Not5p complexes. What elements regulate this balance, and how many different *yTaf_{II}19p* and Not5p complexes there are, are very interesting questions that can now be addressed.

Acknowledgments—We thank Stéphane Jacquier for the purification of recombinant *yTaf_{II}19p* and Nicole Paquet for expert technical assistance in all of the biochemical experiments. We also thank Brice Petit and Caroline Raveraud for technical assistance. We thank Joe Reese and Anthony Weil for *yTaf_{II}* and TBP antibodies, Matthias Mayer for pMPM272, Ursula Oberholzer for strains and plasmids, and Clyde Denis for B42-Ccr4 and B42-Caf1 expression plasmids. We thank members of our laboratory for fruitful discussions.

REFERENCES

- Conaway, R. C., and Conaway, J. W. (1993) *Annu. Rev. Biochem.* **62**, 161–190
- Hernandez, N. (1993) *Genes Dev.* **7**, 1291–1308
- Burley, S. K., and Roeder, R. G. (1996) *Annu. Rev. Biochem.* **65**, 769–799
- Grant, P. A., Schieltz, D., Pray-Grant, M. G., Steger, D. J., Reese, J. C., Yates, J. R., III, and Workman, J. L. (1998) *Cell* **94**, 45–53
- Wieczorek, E., Brand, M., Jacq, X., and Tora, L. (1998) *Nature* **393**, 187–191
- Brand, M., Yamamoto, K., Staub, A., and Tora, L. (1999) *J. Biol. Chem.* **274**, 18285–18289
- Ogryzko, V. V., Kotani, T., Zhang, X., Schiltz, L. R., Howard, T., Yang, X.-J., Howard, B. H., Qin, J., and Nakatani, Y. (1998) *Cell* **94**, 35–44
- Struhl, K., and Moqtaderi, Z. (1998) *Cell* **94**, 1–4
- Hahn, S. (1998) *Cell* **95**, 579–582
- Chen, W., and Struhl, K. (1988) *Proc. Natl. Acad. Sci. U. S. A.* **85**, 2691–2695
- Mahadevan, S., and Struhl, K. (1990) *Mol. Cell. Biol.* **10**, 4447–4455
- Moqtaderi, Z., Bai, Y., Poon, D., Weil, A. P., and Struhl, K. (1996) *Nature* **383**, 188–191
- Moqtaderi, Z., Keaveney, M., and Struhl, K. (1998) *Mol. Cell* **2**, 675–682
- Komarnitsky, P. B., Michel, B., and Buratowski, S. (1999) *Genes Dev.* **13**, 2484–2489
- Birck, C., Poch, O., Romier, C., Ruff, M., Mengus, G., Lavigne, A.-C., Davidson, I., and Moras, D. (1998) *Cell* **94**, 239–249
- Oberholzer, U., and Collart, M. A. (1998) *Gene* **207**, 61–69
- Collart, M. A., and Struhl, K. (1993) *EMBO J.* **12**, 177–186
- Collart, M. A., and Struhl, K. (1994) *Genes Dev.* **8**, 525–537
- Liu, H.-Y., Badarinarayana, V., Audino, D. C., Rappsilber, J., Mann, M., and Denis, C. L. (1998) *EMBO J.* **17**, 1096–1106
- Lee, T. I., Wyrick, J. J., Koh, S. S., Jennings, E. G., Gadbois, E. L., and Young, R. A. (1998) *Mol. Cell. Biol.* **18**, 4455–4462
- Collart, M. A. (1996) *Mol. Cell. Biol.* **16**, 6668–6676
- Benson, J. D., Benson, M., Howley, P. M., and Struhl, K. (1998) *EMBO J.* **17**, 6714–6722
- Wach, A., Brachat, A., Pohlmann, R., and Philippsen, P. (1994) *Yeast* **10**, 1793–1808
- Chevray, P. M., and Nathans, D. (1992) *Proc. Natl. Acad. Sci. U. S. A.* **89**, 5789–5793
- Zervos, A. S., Gyuris, J., and Brent, R. (1993) *Cell* **72**, 223–232
- Klebanow, E. R., Poon, D., Zhou, S., and Weil, A. P. (1997) *J. Biol. Chem.* **272**, 9436–9442
- Cormack, B. P., and Struhl, K. (1992) *Cell* **69**, 685–696
- Yaffee, M. P., and Schatz, G. (1984) *Proc. Natl. Acad. Sci. U. S. A.* **81**, 4819–4823
- Wootner, M., Wade, P. A., Bonner, J., and Jaehning, J. A. (1991) *Mol. Cell. Biol.* **11**, 4555–4560
- Pellman, D., McLaughlin, M. E., and Fink, G. R. (1990) *Nature* **348**, 82–85
- Remacle, J. E., and Holmberg, S. (1992) *Mol. Cell. Biol.* **12**, 5516–5526
- Sanders, S. L., Klebanow, E. R., and Weil, A. P. (1999) *J. Biol. Chem.* **274**, 18847–18850
- Poon, D., Campbell, A. M., Bai, Y., and Weil, A. P. (1994) *J. Biol. Chem.* **269**, 23135–23140
- Alberts, T. K., Lemaire, M., van Berkum, N. L., Gentz, R., Collart, M. A., and Timmers, M. H. T. (2000) *Nucleic Acids Res.* **28**, 809–817
- Hope, I., and Struhl, K. (1986) *Cell* **46**, 885–894